Moon Image Acquisition for Pointing Calibration of LAPAN-A2 Satellite's High Resolution Camera

1st Rosza Madina
Satellite Technology Center
Indonesian National Institute of Aeronautics and Space (LAPAN)
Bogor, Indonesia
rosza.madina@lapan.go.id

2nd Ade Putri Septi Jayani
Satellite Technology Center
Indonesian National Institute of Aeronautics and Space (LAPAN)
Bogor, Indonesia
ade.putri@lapan.go.id

3rd Annisa Sarah
Satellite Technology Center
Indonesian National Institute of Aeronautics and Space (LAPAN)
Bogor, Indonesia
annisa.sarah@lapan.go.id

4th M. Mukhayadi
Satellite Technology Center
Indonesian National Institute of Aeronautics and Space (LAPAN)
Bogor, Indonesia
muh.mukhayadi@lapan.go.id

***Abstract*— The missions of LAPAN-A2 satellite are Earth observation using an RGB digital camera, maritime traffic monitoring, and amateur radio communications. The satellite carries a digital camera, to support the mission, with ground resolution 4 m and a swath width 7 km. It is necessary to do pointing calibration to measure misalignment between spacecraft's attitude sensors, spacecraft axis, and cameras, to make sure the accuracy of the camera pointing when capture the image. By using the inertial pointing method, that the satellite is controlled in three axis to direct the satellite camera to the Moon. Nevertheless, the field of view (FOV) of high-resolution digital cameras is very narrow, which is only 0.7° for the Moon to be fully visible in the camera frame. During image acquisition, the star sensor should be still able to see the star so the attitude information of spacecraft can be well determined. It means the time period and position for Moon acquisition is limited. By capturing multiple images, LAPAN-A2 satellite success to get the Moon images right in the center of the frame within the offset between camera and spacecraft axis are 0.1232° on the *x* axis and -0.93° on the *y* axis.**

***Keywords—LAPAN-A2, pointing calibration, Moon pointing, high-resolution camera** (key words)*

I. INTRODUCTION

LAPAN-A2 satellite is a second microsatellite developed by the Indonesian National Aeronautics and Space Institute (LAPAN). The missions are Earth observation using an RGB digital camera, maritime traffic monitoring, and amateur radio communications [1-5]. The satellite is also referred as LAPAN-ORARI satellite and the amateur radio community call it as IO-86. The satellite was launched on September 28th, 2015 using PSLV C-30 rocket from the Satish Dhawan Space Station, Sriharikota, India on near-equatorial orbit. The satellite carries a high resolution digital camera that has sensor 2048 x 2044 pixels with 4 m ground resolution and 7 km swath width at an altitude of 650 km [6].

To make sure the accuracy of imaging using LAPAN-A2 high-resolution digital camera, it is necessary to do a pointing calibration by measure the alignment between attitude sensor, spacecraft axis and camera. This pointing calibration would improve the mapping of LAPAN-A2 satellite images. As an experimental satellite, LAPAN-A2 has to demonstrate the capability of attitude control which consists of some modes [7]. Those modes are nadir and off nadir pointing mode, interactive control mode, and targets locking mode. Each attitude control mode has been performed on the previous generation satellites based on the momentum bias method [8-12].

Performing pointing calibration by using objects on the Earth's surface is difficult since the satellite projection is moving fast over the ground track with the speed about 6.834 km/s for low Earth orbit within 650 km height [13]. Furthermore, the spacecraft should rotate around 0.06°/s to maintain the pointing toward Earth's center or nadir. Therefore, inaccuracy in a few seconds will make the pointing of camera away from the target. Alternatively, pointing calibration can be executed by exposing satellite's camera towards celestial objects using inertial pointing. One of the interesting targets of celestial objects is the Moon. In addition of giving absolute pointing accuracy for pointing calibration, Moon also a good target for focusing calibration of the camera optical system. However, in the case of the LAPAN-A2 satellite, the diameter of the Moon is only slightly smaller than the swath width of the camera, leaving only a small margin of the camera frame. Thus, the Moon image will only completely visible in the camera frame if the pointing is exactly toward the center of the Moon.

The purpose of this study is to measure the misalignment between star sensor as attitude determination sensor, spacecraft axis, and camera by lunar pointing calibration for improving the pointing accuracy of LAPAN-A2 satellite in high resolution imaging. The acquisition of Moon image can be performed only at certain periods to enable the star sensor to find out the satellite attitude information (star data) when performing pointing calibration. The accuracy of satellite pointing should meet $\leq 0.1°$ to get the perfect full Moon imaging. To support the imaging mission, LAPAN-A2 satellite's equipped by two star sensors that placed as seen in Fig. 1.

LAPAN-A2 satellite's has 2 star sensors which are placed at $+x$ side and $-x$ side within 45° tilting angle from $-z$ side with the expectation the star sensor could get attitude information all the time. However, after the launch and early orbit phase, only star sensor which is placed at $-x$ side could operate nominally. It rises a consequence of limited imaging

978-1-7281-3675-2/19/$31.00 ©2019 IEEE

orientation that is supplemented by attitude information from star sensor. Exceeding a maneuver limit would lead the star sensor at *-x* blinded by the Sun, or blocked by the Earth, so it could not see the stars to determine the satellite's attitude. LAPAN-A2 satellite's star sensor and camera specifications [14-17] are listed in the Table I. The other constraint for pointing calibration using the Moon as a target is about the camera field of view which is only 0.7°. When the pointing angle exceeds the margin of error value, the target would not appear exactly in the center of the frame or even out of the frame, so the frame only shows the dark sky.

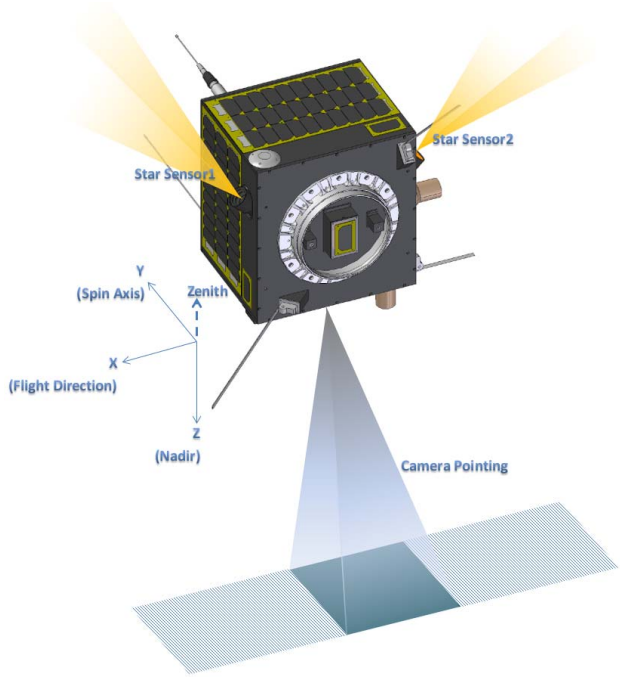

Fig. 1. Star Sensors Placement on LAPAN-A2 Satellite [18]

TABLE I. LAPAN-A2 SATELLITES STAR SENSOR AND HIGH RESOLUTION DIGITAL CAMERA SPECIFICATION

	Star Sensor	**High Resolution Digital Camera**
Sensor	CMOS	CMOS
FOV	14° x 14°	0.7° x 0.7°
Pixel Size	25 µ	5.5 µ
Number of Pixel	512 (H) x 512 (V)	2048 (H) x 2048 (V)
Focal Length	50 mm	1000 mm
Update period	4 Hz	1 Hz (0.9 s repetition)
Power Consumption	2.5 W	7.3 W
Mass	0.820 kg	6 kg

A celestial coordinate system is used for specifying positions of celestial objects. It is analogous to the geographic coordinate system used on the surface of Earth that are projected on the celestial sphere. Nevertheless, since the Moon is not too far from the Earth, it is not really an inertial object. Hence, the Moon position in celestial coordinates depends on the observer position. It means the pointing angle to capture the Moon image would slightly changes related to the movement of the spacecraft. Thus, the pointing angle calculation for Moon image acquisition should use topocentric coordinates instead of geocentric coordinates.

As an object on the celestial sphere, the Moon coordinates are expressed as right ascension (RA) and declination (DE) and azimuth (AZ). The declination measures the angular distance of an object perpendicular to the celestial equator, positive to the north, negative to the south. The right ascension measures the angular distance of an object eastward along the celestial equator from the vernal equinox to the object. While the position of objects in the celestial coordinates is often expressed as a pair of right ascension and declination, this study also takes azimuth in defining the orientation of the Moon. In this study, azimuth is defined as a rotation angle of the object viewed by an observer that measured from true north and increasing westward as defined by Euler Angle of star sensor.

Contrary with geocentric coordinate system that puts the reference point at the center of the Earth, topocentric coordinates use the observer's local horizon as the fundamental plane. Since topocentric coordinates use observer location as reference for defining the celestial object so the positions of the Moon on the celestial sphere depend on the observer's location. It is very easy to see that the geocentric and topocentric coordinates of the Moon differ considerably. The displacement along or above the Earth's surface results in slight shift of Moon image on the celestial sphere. The closer a celestial object to the Earth, the larger its angular offset when moving an observer along the Earth's surface. For a celestial object nearest the Earth, this offset from a geocentric position is called parallax. Fig. 2 illustrate the difference between system coordinate or parallax.

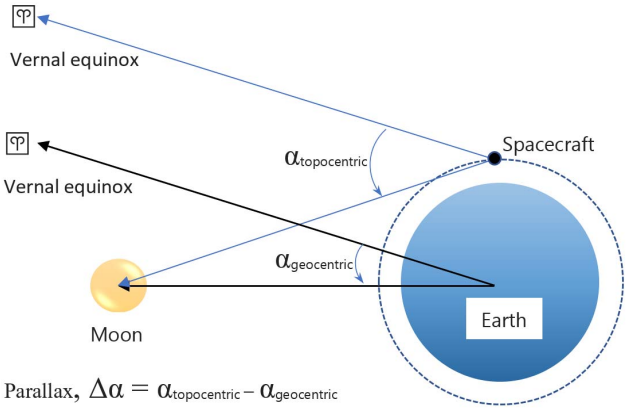

Fig. 2. Illustration of Moon Parallax

For celestial objects observation, especially the Moon, which is located not too far from the Earth, the various reference points would affect different results in the Moon position calculation. Fig. 3 illustrated three observers at different position. Observer A and observer C are in the different hemisphere, while observer B right on the center of the Earth. If geocentric coordinates are used by observer B, then the Moon's position will be right on the reference star's position. In other hand, topocentric coordinates that used by observer A placed the Moon at M'', so does observer C would see the Moon at position M'. Angle α that measured the position of the Moon from the reference star as seen by observer A and observer C is called as Moon parallax. When the Moon is at the zenith of the observer, then the Moon parallax becomes minimum or 0°. Otherwise, it would be maximum when the Moon is on the edge of the observer's horizon.

978-1-7281-3675-2/19/$31.00 ©2019 IEEE

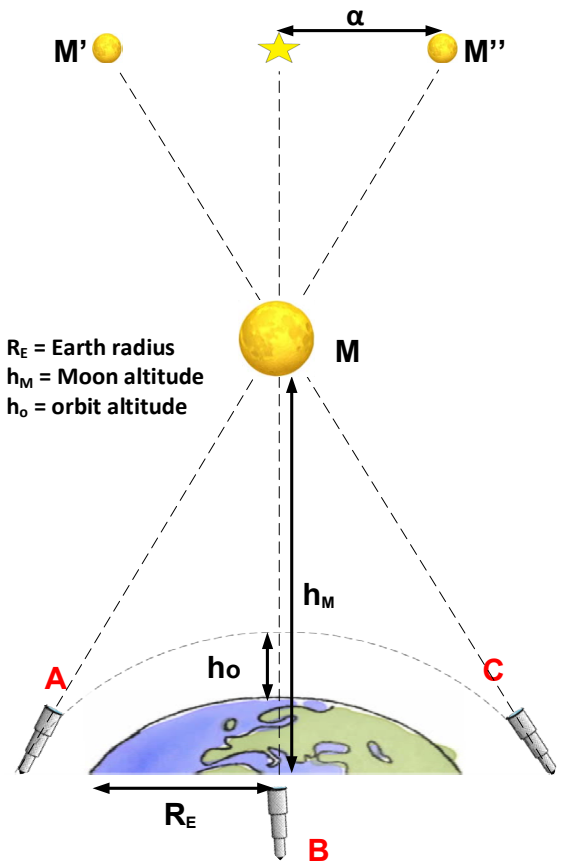

Fig. 3. Difference of Moon Positions Based on Observer Locations

For a simple example, the maximum of Moon parallax that viewed by orbiting spacecraft on 650 km above the Earth's surface can be calculated by following equation.

$$\alpha = \tan^{-1}\left(\frac{R_E + h_o}{h_M}\right) \quad (1)$$

Where: $R_E = 6378.14$ km

$h_M = 384000$ km

The equation found the maximum parallax for Moon image acquisition by the spacecraft within the aforementioned orbit from the geocentric position is about 1.049°. Since the parallax could be greater than the field of view of the camera, ignoring parallax will lead to failure of the Moon imaging.

II. METHODOLOGY

The inertial pointing method is used for satellite maneuver in three axis to orient the satellite's camera to the Moon. In the acquisition of Moon image, star sensor must be in a position to see the stars. Fig. 4 show the geometric relationship between satellite and center of the Earth.

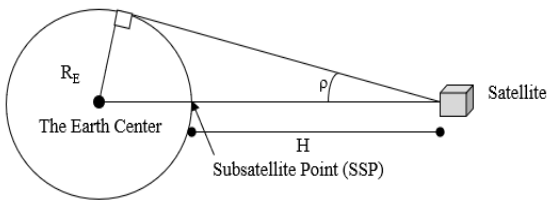

Fig. 4. Relation between Satellite and Center of the Earth

When satellite in the nadir position, the Earth angular radius that visible by the satellite (ρ) from altitude of H can be calculated by following equation.

$$\sin\rho = \frac{R_E}{R_E + H} \quad (2)$$

The equation gives ρ of LAPAN-A2 satellite about 65°. Since the star sensor has a field of view 14°, and tilting angle 45° from -z axis, the minimum pointing angle (η) to capture the Moon will follow the geometric relationship that shown by Fig. 5. Thus, the minimum η can be obtained by following equation.

$$\eta = \rho - \delta \quad (3)$$

Where

$$\delta = STS\ tilting\ angle - half\ of\ STS's\ FoV \quad (4)$$

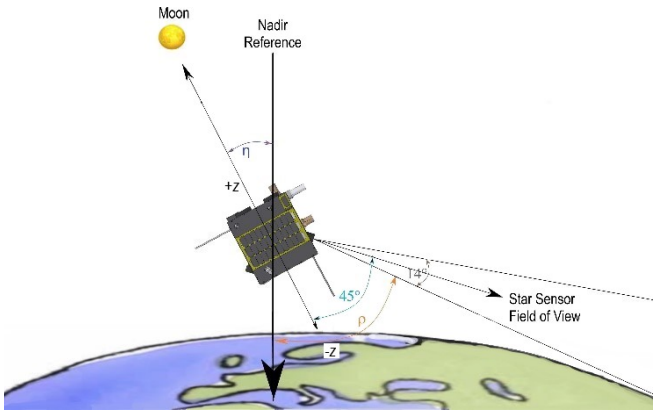

Fig. 5. Angular Relationship between Star Sensor, Spacecraft, and Moon

Those equations give a minimum value of η equal to 27°. It means Moon acquisition can be executed just after it shift 27° from zenith until the Moon is set in the Earth horizon. In addition to the Moon position, the Moon phase must be considered due to the Sun position during the image acquisition. If the Sun has already risen from the horizon in the Moon imaging process, the star sensor will be blinded by the Sun. So the Moon image acquisition should be done before the Moon sets at night or predawn.

The calculation of Moon position in celestial coordinates applies topocentric coordinates by using NASA/JPL DE405 Lunar Ephemeris. The lunar ephemeris data currently are common and available by using the online calculator on the website, so the observer just gives an input of location from where the Moon will be observed [19-20].

III. RESULTS

The pointing calibration using Moon image acquisition has been executed twice: July 23rd and July 26th 2018. The first Moon image acquisition is used to calculate the misalignment between star sensor, spacecraft axis and camera. The misalignment value is then be used to for the second Moon acquisition so the Moon image can fully capture in the frame of LAPAN-A2 satellite's high resolution camera. The first Moon image acquisition setup and lunar ephemeris are listed in the Table II with the results are shown in Fig. 6.

978-1-7281-3675-2/19/$31.00 ©2019 IEEE

TABLE II. LUNAR EPHEMERIS AND THE FIRST ACQUISITION SETUP

Time	2018/07/23 19:41:00 UTC
Spacecraft Position (Lat.; Lon.; Alt.)	5.989868°; 105.542550°; 651.073 km
Spacecraft Zenith (RA; DE; AZ)	-17.7134°; 5.9899°; 89.6263°
Topocentric Lunar Coordinate (RA; DE)	255.2035920°; - 18.936703°
Target of -*z* of Spacecraft (RA; DE; AZ)	75.2036°; 18.9367°; 180°
Actual of -*z* of Spacecraft Provided by STS (RA; DE; AZ)	74.1362°; 18.9104°; 180.198°
Difference between Target and Actual of -*z* (diffRA; diffDE; diffAZ)	1.0674°; 0.0263°; -0.198°

Fig. 6. Results of Moon Image Acquisition on 2018, July 23rd

As shown in Fig. 6, the Moon image in horizontal axis is located at pixel 413 to pixel 1968 in the camera frame, so the Moon diameter consists of 1555 pixels. Since the total pixels of the image are 2048, the dark sky pixels that are not occupied by Moon image equivalent with 493 pixels. On the vertical axis, the top pixel of the Moon is located at pixel 672. The camera placement in the spacecraft is fixed so the horizontal axis is aligned with *x* axis and the vertical axis is aligned to *y* axis of the spacecraft. Since then, the image offset at *x* axis and *y* axis can be defined by following equations.

$$x_{IO} = -\varnothing_M \times \left(\frac{1^{st}\ moon\ pixel\ in\ x\ -\left(dark\ sky\ pixel/_2\right)}{total\ moon\ pixel}\right) \quad (5)$$

$$y_{IO} = -\varnothing_M \times \left(\frac{1^{st}\ moon\ pixel\ in\ y\ -\left(dark\ sky\ pixel/_2\right)}{total\ moon\ pixel}\right) \quad (6)$$

Where:

$\varnothing_M$ = Moon′s angular diameter = 0.49°

x_{IO} = image offset in *x* axis

y_{IO} = image offset in *y* axis

By applying (5) and (6) to the Moon image of Fig. 6, the image offsets are found to be -0.052° on the *x* axis direction and -0.134° on the *y* axis direction.

Since the actual attitude in the Moon acquisition was not perfectly same as the target, then the calculation of the camera offset should accommodate the difference between actual and target of the spacecraft attitude. In the Moon imaging setup, the azimuth was arranged so rotation about *x* axis will change DE, and *y* rotation will change RA. Therefore, the camera offset on the *x* and *y* axis can be established by using equations below.

$$x_{CO} = -x_{IO} - DiffDE \quad (7)$$

With

$$DiffDE = DE_{target} - DE_{actual} \quad (8)$$

$$y_{CO} = -y_{IO} - DiffRA \quad (9)$$

With:

$$DiffRA = RA_{target} - RA_{actual} \quad (10)$$

Where:

x_{CO} = camera offset in *x* axis

y_{CO} = camera offset in *y* axis

By using those equations, the first Moon imaging lead to find the camera offsets 0.03° on the *x* axis and -0.93° on the *y* axis. Then these values have been implemented for second Moon imaging, which has ephemeris as listed in the Table III. The results of the second Moon image acquisition are displayed in the Table IV.

TABLE III. LUNAR EPHEMERIS IN THE SECOND ACQUISITION

Time	2018/07/26 22:36:00 UTC
Spacecraft Position (Lat.; Lon.; Alt.)	1.013118°; 113.545953°; 646.453 km
Spacecraft Zenith (RA; DE; AZ)	37.1167°; 1.0131°; 84.0840°
Topocentric Lunar Coordinate (RA; DE)	294.7202970°; -20.166477°
Target of -*z* of Spacecraft (RA; DE; AZ)	113.7803°; 20.1965°; 180.0000°

According to the Table IV, it appears that the Moon is fully captured at picture index 4. In that picture, diffRA gives reasonable value or close to zero, that is 0.0644°, so y_{CO} is perfectly matched. However, diffDE in the picture 4 is still not matched so x_{CO} has to be updated. Meanwhile, the diffDE on picture 3 give the best result since the Moon position is exactly in the center of *x*. Looking back at the first image obtained of the Moon (Fig. 6), a mismatch might occur because the Moon is not a full Moon, so the pixel measurement might not so accurate. Thus, the image offset of picture 3 should be 0, so the equation 7 is used to correct the value of x_{CO} as following.

$$x_{CO\_new} = -diffDE_{picture\_3} \quad (11)$$

$$= 0.1232°$$

The updated value of the camera offset (x_{CO} = 0.1232°) can be verified by comparing the Moon picture in the Table IV with the image offset (x_{IO}) that recalculated from equation (7) using the new x_{CO}. Table V displayed the value of the image offset for every picture index of the Table IV. Since the diffDE of picture 3 is used as reference for updating the offset on the *x* axis, the image offset should result 0. The smaller image offset means the closer Moon image from the center of axis, and it has been confirmed by the Table V.

TABLE IV. RESULTS OF MOON IMAGE ACQUISITION MEASUREMENT ON 2018, JULY 26TH

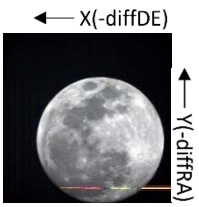	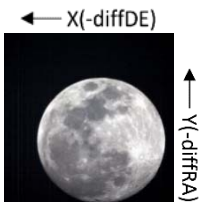	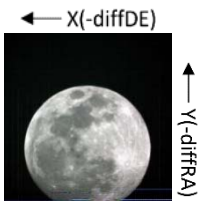	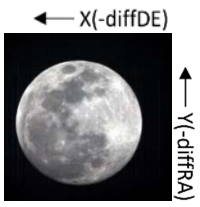	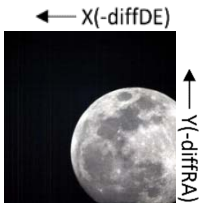
picture index: 1	picture index: 2	picture index: 3	picture index: 4	picture index: 5
diff RA: 0.1420	diff RA: 0.1420	diff RA: 0.1469	diff RA: 0.0644	diff RA: 0.1047
diff DE: -0.1025	diff DE: -0.1025	diff DE: -0.1232	diff DE: -0.1442	diff DE: 0.1456
diff AZ: 1.3768	diff AZ: 1.3768	diff AZ: 1.3923	diff AZ: 1.4098	diff AZ: 1.2278

TABLE V. VALUE OF IMAGE OFFSET OF TABLE IV

X_{IO} of picture index: 1	X_{IO} of picture index: 2	X_{IO} of picture index: 3	X_{IO} of picture index: 4	X_{IO} of picture index: 5
-0.0207	-0.0207	0	0.021	-0.2688

To prove the accurate sensor pointing calibration, the Earth imaging has been conducted afterward. The Earth imaging test after pointing calibration was done coincide with the call for disaster mitigation due to an earthquake. At that time, many tourists were trapped on the summit of Mount Rinjani due to avalanches when a 6.4-magnitude earthquake struck the Indonesian tourist island of Lombok on July 29th, 2018. Rescuers set off one day later to help nearly 700 trekkers and climbers who became stranded at two points on the mountain, after landslides caused by the earthquake blocked some trails off the peak [21].

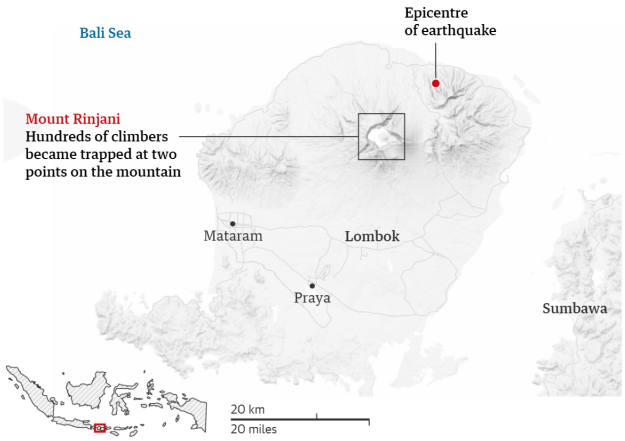

Fig. 7. Lombok Earthquake on July 29th, 2018 [21]

LAPAN-A2 satellite had the opportunity to capture the summit of Mount Rinjani on August 2nd and 3rd, 2018, to find out if there was a deformation on the peak of the mountain after the earthquake. The resulting images of high-resolution camera on those two consecutive days have demonstrated a very high accuracy pointing of the LAPAN-A2 satellite.

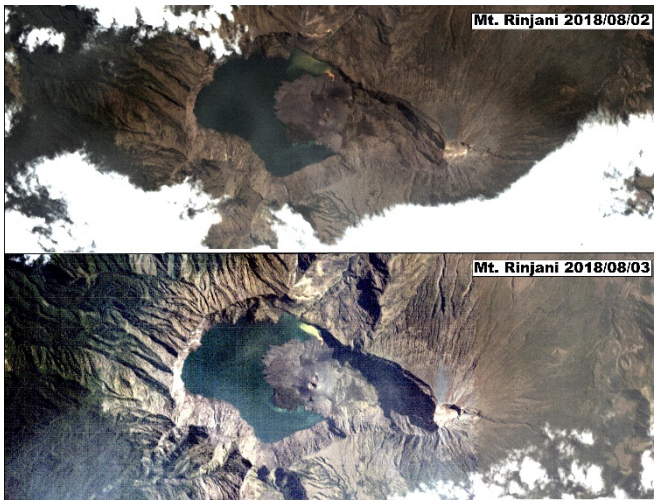

Fig. 8. Pointing Test in the Mount Rinjani Imaging

IV. CONCLUSION

LAPAN-A2 satellite has successfully captured Moon image exactly in the center of its high-resolution camera frame. This Moon image acquisition for pointing calibration has been done by using the Moon ephemeris that applied topocentric coordinates. Offset value for image acquisition using LAPAN-A2 satellite's high-resolution camera based on the result of pointing calibration is 0.1232° on the *x* axis and -0.93° on the *y* axis. These offset values can be used to improve the image acquisition on the Earth's surface. In the future, this method is promising to be used to observe other celestial objects or for focusing calibration of the camera's optical system using the Moon.

REFERENCES

[1] S. Hardhienata, R.H. Triharjanto and M. Mukhayadi, "LAPAN-A2: Indonesian near-equatorial surveilance satellite," 18th Asia-Pacific Regional Space Agency Forum (APRSAF), 2011.

[2] W. Hasbi and A. Karim, "LAPAN-A2 System Design for Equatorial Surveillance Missions," Small Satellites for Earth Observation : Missions & Technologies, Operational Responsive Space, Commercial Constellations, International Academy of Astronautics, 2014

[3] C.T. Judianto and A. Wahyudiono, "Automatic Identification System and Surveillance Technology for Indonesia Marine Security on LAPAN-A2 Satellite," International Seminar of Aerospace Science and Technology, 2014.

[4] W. Hasbi, Kamirul, M. Mukhayadi, U. Renner, "The Impact of Space-Based AIS Antenna Orientation on In-Orbit AIS Detection Performance," Appl. Sci. 2019, 9, 3319.

[5] M. Mukhayadi, A. Karim, W. Hasbi, R. Permala, "Designing a Constellation for AIS mission based on data acquisition of LAPAN-A2 and LAPAN-A3 Satellites," Telkomnika Indones. J. Electr. Eng. 2019, 17, 1774–1784.

[6] A. Wahyudiono and R. Madina, "Utilization of Digital Camera Payload on LAPAN-A2 Satellite for Monitoring of Toll Road Construction in Java Island," Seminar Nasional Iptek Penerbangan dan Antariksa, 2017.

[7] A.H. Syafrudin, W. Hasbi, and A. Rahman, "Camera Payload Systems For The LAPAN A2 Experimental Microsatellite," Proceedings of ACRS, 2013.

[8] M. Steckling, U. Renner and H.P. Röser, "DLR-TUBSAT, qualification of high precision attitude control in orbit," Acta Astronautica, 1996, 39, 951-60.

[9] R. H. Triharjanto, W. Hasbi, A. Widipaminto, M. Mukhayadi, U. Renner, "LAPAN-TUBSAT: Micro-Satellite Platform for Surveillance & Remote Sensing," Proceedings of the 4S symposium: Small Satellites, Systems and Services, September 2004.

[10] T. Mediansyah and M. Mukhayadi, "Implementation of Target Locking Method on LAPAN Tubsat Satellite Using Speed Angle Profile," Satelit Mikro Untuk Mitigasi Bencana Dan Ketahanan Pangan, IPB Press, June 2010.

[11] M. Mukhayadi, R. Madina, and U. Renner, "Attitude control of bias momentum micro satellite using magnetic and gravity gradient torque," IEEE International Conference on Aerospace Electronics and Remote Sensing Technology, 2014.

[12] S. Utama, M. A. Saifudin and M. Mukhayadi, "Momentum Biased Performance of LAPAN-A3 Satellite for Multispectral Pushbroom Imager Operation," IOP Conference Series: Earth and Environmental Science, Vol. 149, 2018.

[13] J.R. Wertz and W. Larson, "Space Mission Analysis and Design," 3rd Edition published by Microcosm Press and Kluwer Academic Publishers, 1999.

[14] M. A. Saifudin and M. Mukhayadi, "Sistem Attitude Determination and Control (ADCS) Satelit LAPAN-A2/Orari," Media Dirgantara, 2015.

[15] M. Buhl and U. Renner, "Star Sensor Development Based on the TUBSAT Experience," in Small Satellite Missions for Earth Observation, Springer Berlin Heidelberg, 2010.

[16] A. H. Syafrudin, W. Hasbi, A. Rahman, "Camera Payload Systems for the LAPAN A2 Experimental Microsatellite", Proceedings of Asian Conference on Remote Sensing, 2013.

[17] C. A. Rokhmana, E. Novalinda, "Geometric Correction on Raw Data Image of Spacecam LAPAN-A2 Satellite for Visual Interpretation", Prosiding Seminar Nasional Penginderaan Jauh, 2017.

[18] M. A. Saifudin, M. Mukhayadi, "LAPAN-A2 Attitude Control Strategy for Equatorial Surveillance Mission," Proceedings of the 9th IAA Symposium on Small Satellites for Earth Observation, Berlin, Germany, April 8-12, 2013.

[19] JPL Planetary and Lunar Ephemerides
https://ssd.jpl.nasa.gov/?planet_eph_export
accessed 2018, July 23rd.

[20] DE405 Lunar Ephemeris Calculator
http://www.neoprogrammics.com/Moon/DE405_Lunar_Ephemeris_Calculator.php
accessed 2018, July 23rd.

[21] K. Lamb (30 July 2018). "Lombok Earthquake: 500 Trapped Climbers Make Way Down Indonesian Peak," The Guardian. Retrieved 2019, September 17th.

978-1-7281-3675-2/19/$31.00 ©2019 IEEE